NJC

ROYAL SOCIETY OF CHEMISTRY

PAPER

View Article Online
View Journal | View Issue

Cite this: *New J. Chem.*, 2023, **47**, 17491

Counterintuitive noncovalent interactions of ammonia with the all metal ring of cyclic trinuclear Ag(I) clusters: a DFT study†

Athanassios C. Tsipis

Received 22nd July 2023,
Accepted 31st August 2023

DOI: 10.1039/d3nj03420h

rsc.li/njc

Density functional theory electronic structure calculations were employed to study a proposed novel type of interaction between NH_3 and the metallic ring of cyclic trinuclear Ag(I) clusters of the general formula *cyclo*-$Ag_3(\mu_2\text{-}L)_3$ bearing 15 different bridging organic ligands L. Scan single point energy calculations revealed that the most stable orientation of NH_3 is that with a N atom facing the center of the silver metallic ring and bridging the three metal centers. Starting with this orientation we performed geometry optimizations of the *cyclo*-$Ag_3(\mu_2\text{-}L)_3(\mu_3\text{-}NH_3)$ complexes. The optimized geometries retain the initial orientation of NH_3. The zero point energy corrected interaction energies, D_0, of NH_3 with the metallic ring are found in the range 4.2–12.4 kcal mol^{-1} while the distance of NH_3 from the center of the ring is in the range 2.317–2.519 Å, both indicative of a relatively strong interaction. A multitude of theoretical methods employed revealed that the interaction of NH_3 with the silver metallic ring is mainly of ionic nature with a contribution of van der Waals forces. Molecular structure–property relationships indicate that the magnitude of D_0 increases upon increasing the charge of the silver metal centers and decreasing the LUMO energy of the *cyclo*-$Ag_3(\mu_2\text{-}L)_3$ clusters.

1. Introduction

Weak noncovalent interactions are of paramount importance in many research areas such as in molecular biology,[1–3] chemical and biological recognition,[4,5] crystal engineering[6,7] and supramolecular chemistry.[8,9] There are numerous types of noncovalent interactions including H-bonding,[10,11] π···π stacking,[12] cation···π,[13] anion···π,[14] CH···π,[15,16] NH···π,[17,18] and even OH···π, FH···π, and BH···π.[19] XH···π (X = C, N, O, *etc.*) interactions refer to the interaction of the X–H bond facing a perpendicular aromatic ring.[19] Among the XH···π interactions, the most widely studied[20,21] are the CH···π and OH···π interactions while the NH···π interactions are less well studied. Hobza *et al.*[22] studied theoretically the interaction of benzene with NH_3, H_2O and CH_4 and found that the strength of the NH···π interaction lies between those found for CH···π and OH···π interactions. Tsuzuki *et al.*,[17] upon employing *ab initio* calculations, demonstrated the importance of the electrostatic and dispersion interactions in the adducts formed between benzene molecules and water, ammonia or methane. In this study, various different orientations of ammonia relative to the benzene molecule were taken into account and among them the most stable is found to be that where one N–H bond is perpendicular to the benzene ring facing its center. The dispersion forces are the main component of the interaction energy while electrostatic forces govern the orientation of ammonia relative to benzene.[17]

Another less studied noncovalent interaction is the so called lone pair···π (lp···π), which is a bonding interaction between a lone pair and a π system.[23] The lp···π interaction was introduced by Egli *et al.*[24] to explain the contradicting stability of the Z-DNA conformation where O_4' of cytidine 'sits' above the six membered ring of guanine at the d(CpG) steps. The lone pair of the O_4' faces the π system of guanine thus giving rise to an n → π* interaction. The nature of the latter is counterintuitive and cannot be explained based only on simple electrostatic interactions. The elusive nature of the lp···π interaction may involve molecular orbital interactions along with electrostatic ones. Fomine *et al.*,[25] employing LMP2 *ab initio* calculations, demonstrated that, depending upon the electronegativity of the aromatic system, a water molecule should form either an OH···π or an lp···π interaction. The latter involves the interaction of the HOMO of the water molecule with the π* orbitals of the aromatic system. The magnitude of the lp···π interaction can be as high as that of a strong H-bond, especially in the case where the aromatic system is positively charged. Accordingly, the interaction energy between a water molecule and a positively charged imidazole ring

Laboratory of Inorganic Chemistry, Department of Chemistry, University of Ioannina 45110, Greece. E-mail: attsipis@uoi.gr

† Electronic supplementary information (ESI) available. See DOI: https://doi.org/10.1039/d3nj03420h

was calculated to be as high as −8.1 kcal mol^{-1} at the MP2/6-31+G** level of theory.[23]

To date, the largest body of the work on the lp···π interaction was devoted to biomolecules such as DNA, RNA, and proteins as well as materials and small molecules.[26] The most common lp···π interactions studied so far were those related to the interactions of an aromatic system with O and N lone pairs.[27]

To the best of our knowledge, all the studies of the lp···π interaction have been limited to systems where the lone pair faces a π organic ring. In contrast, there are no such studies focusing on the interaction between a lone pair and an all-metal ring. It is noticed that various ligand stabilized all metal rings have been proposed to exhibit the so-called metallaromaticity phenomenon.[28] In these systems, there exist molecular orbitals (MOs) delocalized over the entire metallic ring similar to the delocalized MOs found for aromatic organic rings. Cundari *et al.*[29] employed DFT calculations at the B3LYP/CEP-31G(d) level of theory to study the π-acid/base – properties of cyclic trinuclear complexes of monovalent coinage metals of the formula *cyclo*-$M_3(\mu\text{-}L)_3$. Depending upon the interplay of the ligand, metal and substituents, *cyclo*-$M_3(\mu\text{-}L)_3$ exhibits either π-basicity or π-acidity which in some cases is superior to those estimated for various organic π-systems, *e.g.* benzene, pyridine, pyrazol, *etc.* It should also be noticed that the cyclic trinuclear complexes can participate in π stacking interactions with π organic molecules. Accordingly, Balch *et al.*[30] demonstrated that the cyclic trinuclear Au(I) complex, $Au_3(MeN{=}COMe)_3$, forms stacking compounds with nitro-9-fluorenones. In these compounds, the trinuclear Au(I) metallic ring faces, in a parallel fashion, the organic rings of nitro-9-fluorenones forming charge transfer adducts. The ability of cyclic trinuclear coinage metal complexes to form π stacking supramolecular systems with organic π molecules was revealed in a number of studies by Dias *et al.*[31] More specifically, the cyclic trinuclear $\{[3,5\text{-}(CF_3)_2\text{-}Pz]Au\}_3$ complex forms π stacks with toluene while the cyclic trinuclear $\{[3,5\text{-}(CF_3)_2Pz]Ag\}_3$ cluster forms π-acid–base adducts with benzene and substituted benzenes. In other studies,[32] it was shown that the cyclic trinuclear Au(I) compounds could form π stacking supramolecular assemblies with the cyclic trinuclear Hg(I), *cyclo*-$Hg_3(\mu\text{-}C_6F_5)$ complex. The latter is considered to be a strong π-acid that could form 1 : 1 π-acid–base stacking compounds with various arenes.[33] In addition, the cyclic trinuclear Au(I) complexes could interact with Tl(I) or Ag(I) cations as well as organic π-acids, *e.g.* C_6F_6 and the TCNQ molecule forming π stacks.[32]

Also, the importance of the interactions of ammonia with various species is exemplified in MOFs used as ammonia storage materials. In the latter, ammonia interacts with either the organic linkers or the open metal sites.[34–39]

Taking into account all the above mentioned ammonia interactions, as well as their implications in ammonia storage in MOFs, we thought it would be advisable to study theoretically the interaction of ammonia with various cyclic trinuclear Ag(I) clusters of the general formula *cyclo*-$Ag_3(\mu_2\text{-}L)_3$ by means of DFT electronic structure calculations. Our aims were (i) to reveal if NH_3 could interact with metallic rings, (ii) what would be the orientation of ammonia relative to the metallic rings, (iii) what is the strength of this interaction and how is this affected by the bridging ligands L, and finally (iv) to delineate the nature of this interaction.

2. Computational details

All calculations were performed using the Gaussian09 version D.01 program suite.[40] Geometry optimizations were performed without symmetry constrains, employing the 1997 hybrid functional of Perdew, Burke, and Ernzerhof (PBE0)[41] along with the Def2-TZVP basis set.[42] Dispersion interactions were accounted by using the D3 version of Grimme dispersion with Becke–Johnson damping.[43] The computational protocol will be hereafter denoted as PBE0-GD3BJ/Def2-TZVP. All stationary points have been identified as minima (the number of imaginary frequencies, NImag = 0). Natural bond orbital (NBO) population analysis was done employing the methodology by Weinhold.[44] The atoms in molecules (AIM) of Bader[45] and the reduced gradient density (RDG) method[46] were used as implemented in the Multiwfn software.[47]

3. Results and discussion

3.1 Structural data

3.1.1 Orientation of the NH_3 molecule. The six possible orientations of the NH_3 molecule relative to the cyclic trinuclear metallic ring of the *cyclo*-$[Ag_3(\mu_2\text{-}L)_3]$ clusters are depicted in Scheme 1. Initially, we performed a rigid scan of the potential energy hypersurface, PES, for all six conformations, **A–F**, by only changing the distance of the ammonia molecule from the center of the metallic ring (**A–D**) or from the middle of a Ag–Ag

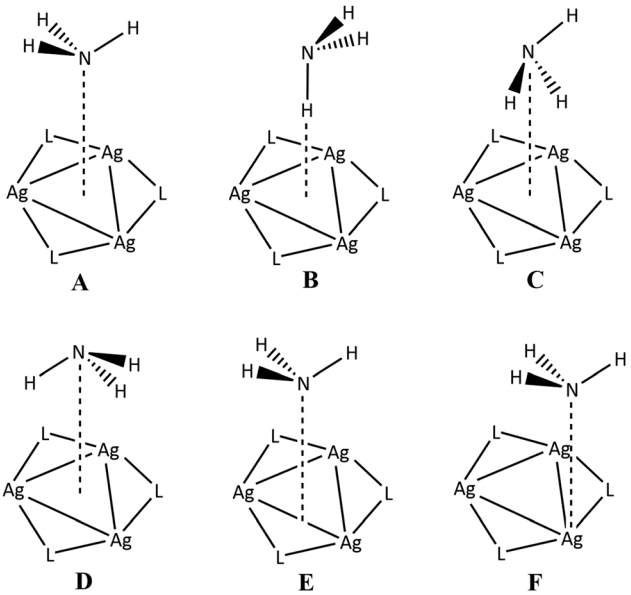

Scheme 1 Possible orientations of NH_3 relative to the silver(I) metallic clusters.

bond (**E**) or from a Ag metal center (**F**), while keeping all the rest of the structural parameters frozen.

Fig. 1 depicts the scan curves for two representative complexes with NH_3, namely the *cyclo*-{$Ag_3[\mu_2$-(1*H*-tetrazole)$]_3$}, **1**, and the *cyclo*-{$Ag_3[\mu_2$-(3,5-bis-trifluoromethyl-1*H*-1,2,4-triazole)$]_3$}, **2**. Perusal of Fig. 1 reveals that in both **1** and **2** the most stable is conformation A. Table 1 shows the relative stabilities of all conformations calculated for **1** and **2**. Similar scan curves are obtained for the rest of NH_3 complexes under study.

Inspection of Table 1 reveals that conformations **B–F** are less stable by about 0.8–6.6 kcal mol^{-1} with respect to the most stable conformation A.

3.1.2 Structural and energetic parameters. Taking into account the above mentioned results, we proceed with the full geometry optimizations of a series of Ag(I) cyclic trinuclear complexes with the general formula *cyclo*-$[Ag_3(\mu_2\text{-L})_3(\mu_3\text{-}NH_3]$. Taking into account that conformation **A** of these clusters is the most stable (*vide supra*), we started our calculations with NH_3 located exactly above the centre of the metallic ring as in conformation **A** (Scheme 1). The bridging ligands, L, of the clusters under study are depicted in Scheme 2.

Table 1 Relative stabilities (in kcal mol^{-1}) of the conformations **A–F** calculated for **1** and **2** at the PBE0-GD3BJ/Def2-TZVP level of theory

Conformation	1	2
A	0.0	0.0
B	6.6	6.4
C	6.4	6.3
D	6.1	5.7
E	2.7	0.8
F	2.8	1.7

Fig. 2 also depicts the optimized geometries of a few representative complexes (**1** and **2**). The optimized structures of the rest of the complexes under study are given in Fig. S1–S3 of the ESI.†

The most important structural parameters of the optimized geometries of complexes **1–15** are given in Table 2. These are, the distance between the N atom of ammonia and a centroid, cd pseudoatom located at the centre of the metallic ring, R_e(N-cd), and the intermetallic Ag–Ag distance, R_e(Ag–Ag) (Scheme 2). It should be noticed that in all cases <N-cd-Ag is

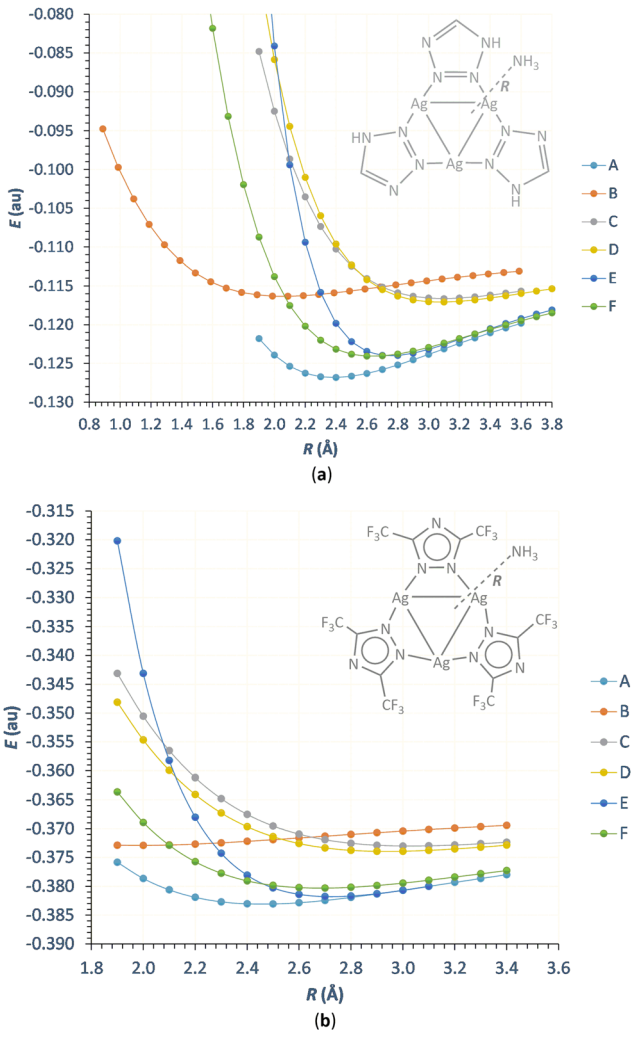

Fig. 1 Rigid scan curves of the distance *R* between NH_3 and the *cyclo*-{$Ag_3[\mu_2$-(1*H*-tetrazole)$]_3$} (a) and the *cyclo*-{$Ag_3[\mu_2$-(3,5-bis-trifluoromethyl-1*H*-1,2,4-triazole)$]_3$} (b) calculated at the PBE0-GD3BJ/Def2-TZVP level of theory.

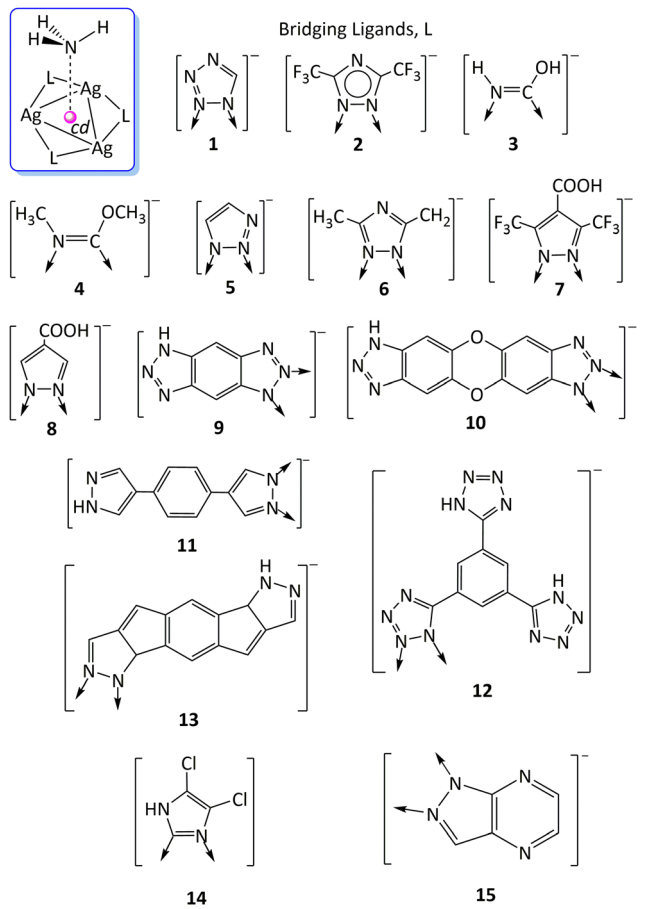

Scheme 2 Bridging ligands, L considered in this study. Donor atoms are indicated with arrows.

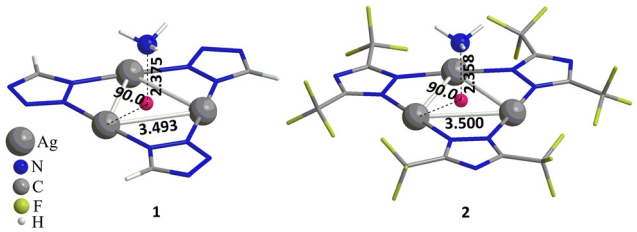

Fig. 2 Optimized geometries of **1** and **2** at the PBE0-GD3BJ/Def2-TZVP level of theory.

Table 2 Structural and energetic parameters of complexes **1–15** calculated at the PBE0-GD3BJ/Def2-TZVP level of theory

Complex	R_e(N-cd) (Å)	R_e(Ag–Ag) (Å)	D_0 (kcal mol^{-1})
1	2.399	3.493	8.7
2	2.358	3.500	9.7
3	2.445	3.432	4.6
4	2.519	3.329	4.2
5	2.385	3.454	7.4
6	2.362	3.438	7.0
7	2.346	3.415	9.7
8	2.328	3.422	7.9
9	2.328	3.452	12.2
10	2.317	3.451	12.4
11	2.356	3.419	7.3
12	2.394	3.512	9.0
13	2.352	3.422	7.2
14	2.391	3.543	5.2
15	2.350	3.466	7.7

90° while the metallic rings form equilateral triangles. The optimization procedure yielded local minima which correspond to conformation **A**. The R_e(N-cd) distance, depending upon L, is found in the range of 2.317–2.519 Å while the R_e(Ag–Ag) distance is in the range of 3.329–3.500 Å. In addition, in Table 2, the interaction energies of the ammonia molecule with the metallic clusters are shown. These correspond to the bond dissociation energies, D_0, of ammonia from the metallic cluster (zero point energies included). The D_0 is found in the range of 4.2–12.4 kcal mol^{-1}. Both the R_e(N-cd) distance and the D_0 indicate that the interaction of ammonia with the silver metallic ring is relatively strong.

3.2 Bonding analysis

3.2.1 Atoms in molecules and reduced density gradient analysis. Taking into account the strength of the ammonia–the metallic ring interaction we instigated to perform bonding analysis by means of the atoms in molecules (AIM) method and the reduced density gradient (RDG) function. The bond critical points (BCPs) found are depicted schematically in Fig. 3 for the representative complexes **1** and **2**. Inspection of Fig. 3(a) reveals that there are three BCPs (denoted as a, b and c) between ammonia and the metallic ring. Actually, these BCPs are located in the midpoints between the N atom and each Ag(I) metallic centre, forming an equilateral triangle. Similar BCPs are also found for the rest of the complexes under study namely **3–15**. The existence of these BCPs is indicative of bonding interactions between ammonia and the metallic Ag(I) clusters.

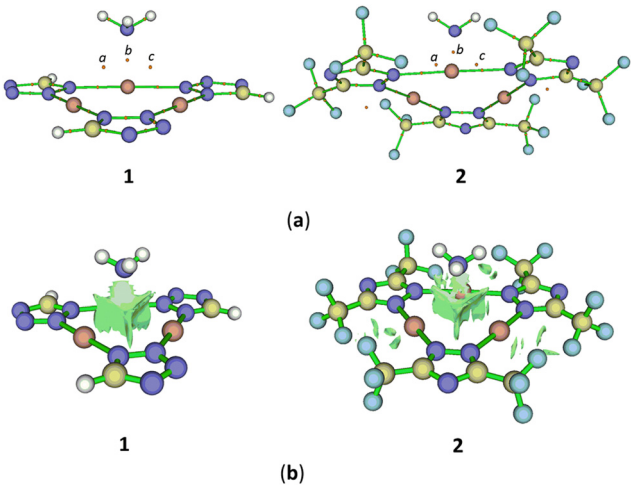

Fig. 3 BCPs (a) and 3D plot of the RDG function (b) for **1** and **2**.

Also, in Fig. 3(b), the 3D surface of the RDG function is depicted. The green colour of the RDG indicates that the ammonia–metallic cluster interaction is of van der Waals type.[47]

This is further corroborated upon the inspection of the scatter graph plots of **1** and **2**, as depicted in Fig. 4, of RDG *vs.* sign(λ_2)ρ, where λ_2 is a function obtained as the second largest eigenvalue of the averaged electron density Hessian matrix computed throughout the dynamical trajectory and ρ is the electron density. Similar scatter RDG *vs.* sign(λ_2)ρ graphs are obtained for the rest of the complexes under study.

According to the noncovalent interaction method[48] (NCI), the existence of 'spikes' in the region of −0.01 to 0.01 of sign(λ_2)ρ indicates a van der Waals interaction. In order to further delineate the bonding between ammonia and the metallic cluster we have calculated, a number of parameters at the BCPs a, b and c namely the electron density, ρ_{BCP}, the Laplacian of the electron density, $\nabla^2\rho_{BCP}$, the potential energy density, V_{BCP}, the kinetic energy density, G_{BCP}, and the energy density, H_{BCP}. Espinoza[49] classified the bonding interactions into three categories based on the values of these parameters at the relevant BCPs. Accordingly, if $|V_{BCP}|/G_{BCP} < 1$, $\nabla^2\rho_{BCP} > 0$ and $H_{BCP} > 0$, the interaction is characterized as pure-closed shell (*e.g.* ionic bonds, hydrogen bonds, and van der Waals interactions). If $|V_{BCP}|/G_{BCP} > 2$, $\nabla^2\rho_{BCP} < 0$ and $H_{BCP} < 0$ then, the interaction is characterized as pure open-shell (covalent) and finally if $1 < |V_{BCP}|/G_{BCP} < 2$, $\nabla^2\rho_{BCP} > 0$ and $H_{BCP} < 0$ is of the intermediate nature. The values of all the above mentioned parameters at BCPs a, b and c are given in Table S1 of the ESI.† Perusal of Table S1 (ESI†) confirms that the ammonia–metallic cluster interaction is of closed shell ionic type since in all cases, it is found that at the bonding BCPs, the conditions $|V_{BCP}|/G_{BCP} < 1$, $\nabla^2\rho_{BCP} > 0$ and $H_{BCP} > 0$ are met.

3.2.2 Molecular electrostatic potentials. Fig. 5 depicts schematically the 3D surfaces of the molecular electrostatic potentials (MEPs) of representative silver metallic clusters included in the respected complexes with ammonia along with the MEP of the ammonia molecule. The MEPs of the silver metallic

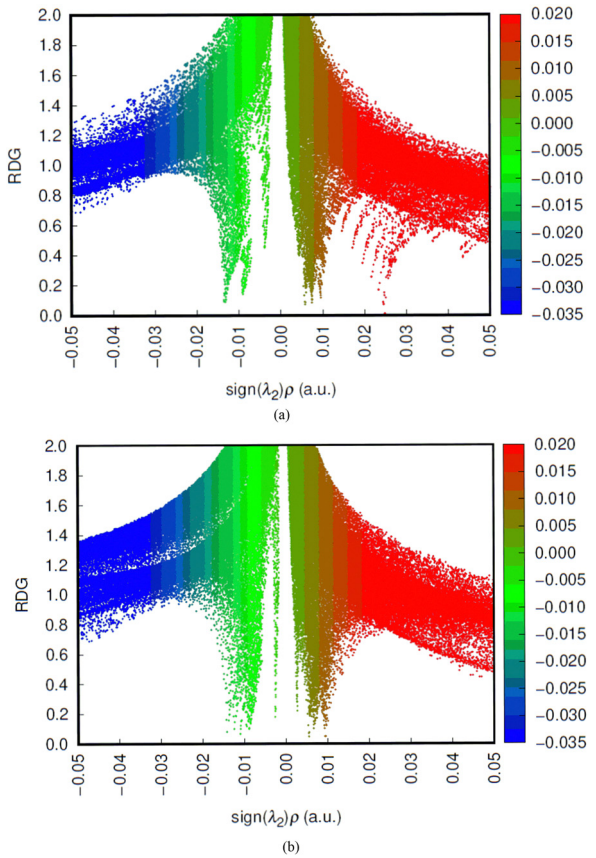

Fig. 4 Scatter graph plots of RDG *vs.* sign(λ_2)ρ for complexes **1** (a) and 2 (b).

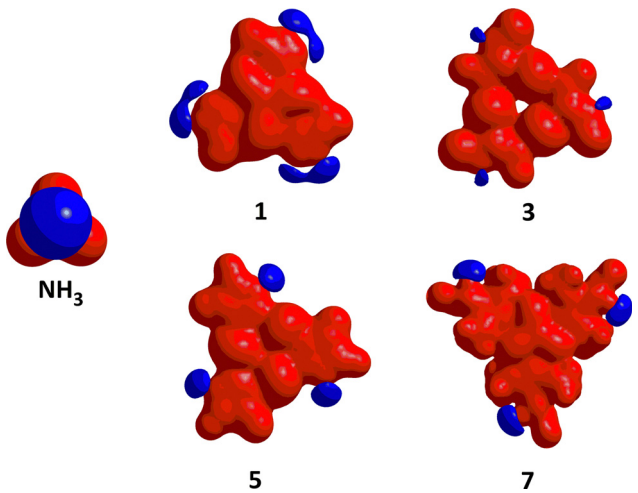

Fig. 5 MEP surfaces of NH_3 and representative silver metallic clusters included in complexes **1**, **3**, **5** and **7**.

clusters included in complexes with ammonia, **1**, **3**, **5** and **7**, exhibit a positive surface (red colour, Fig. 5). The same also holds true for the rest of the complexes under study. On the other hand, the MEP of ammonia exhibits a negative surface (blue colour, Fig. 5) protruding the N atom as a result of its lone pair. Accordingly, based on MEPs, ammonia is expected to favourably interact with the silver metallic ring bearing positive MEP.

3.3 Electronic structures

3.3.1 Natural bond orbital analysis. Next, we employed natural bond orbital (NBO) analysis to find the electron density partitioning of the systems under study. Table 3 presents the natural charges on the ammonia N atom, q_N, and on the Ag metal center, q_{Ag}, and the natural electron configuration (nec) of these atoms, nec(N) and nec(Ag), as obtained from the NBO analysis of **1–15**.

It can be seen from Table 3 that the N atom of ammonia acquires negative charges from −1.048 to −1.094 while the Ag metal centres acquire positive charges from 0.400 to 0.638. Clearly, there is an electrostatic/ionic interaction since the negatively charged N atom of ammonia faces three positively charged Ag cations. From the necs given in Table 3, it can be seen that there is no charge transfer between the ammonia N atom and the metallic cluster.

3.3.2 Molecular orbitals. Fig. 6 depicts the most important MOs for a few representative complexes namely 3 and 10 exhibiting the lowest and the highest D_0, respectively (Table 2).

In Fig. 6 we observe three bonding MOs for **3** and two bonding MOs for **10** indicating a covalent interaction between the sp^3 hybrid bearing the lone pair with d AOs located on the silver metal centers. However, it should be emphasized that despite the existence of these MOs, the covalent interaction between ammonia and the silver metallic ring is expected to be negligible. The latter is further corroborated by the fact that the Wiberg bond indices between the N atom of ammonia and the three silver metals of the ring amount to only 0.090 for **3** and 0.126 for **10**. The same also holds true for the rest of the complexes under investigation, *i.e.* the respective Wiberg bond indices are quite small.

3.4 Molecular structure–property correlations

From Table 2 it is obvious that the strength of the interaction between ammonia and the silver metallic ring depends upon the nature of the bridging ligand. In other words, D_0 depends upon the molecular structure of the silver clusters. Since D_0 is of central importance, we set out to extract molecular structure–property correlations in order to find which factors

Table 3 NBO analysis of complexes **1–15** at the PBE0-GD3BJ/Def2-TZVP level of theory

Species	q_N	q_{Ag}	nec(N)	nec(Ag)
1	−1.072	0.622	$2s^{1.49}2p^{4.56}3p^{0.01}3d^{0.01}$	$5s^{0.45}4d^{9.81}5p^{0.11}$
2	−1.066	0.626	$2s^{1.49}2p^{4.56}3p^{0.01}3d^{0.01}$	$5s^{0.41}4d^{9.83}5p^{0.14}$
3	−1.061	0.400	$2s^{1.48}2p^{4.56}3p^{0.01}3d^{0.01}$	$5s^{0.66}4d^{9.78}5p^{0.16}$
4	−1.048	0.400	$2s^{1.48}2p^{4.55}3p^{0.01}3d^{0.01}$	$5s^{0.63}4d^{9.79}5p^{0.18}$
5	−1.068	0.608	$2s^{1.49}2p^{4.56}3p^{0.01}3d^{0.01}$	$5s^{0.47}4d^{9.81}5p^{0.12}$
6	−1.061	0.575	$2s^{1.48}2p^{4.56}3p^{0.01}3d^{0.01}$	$5s^{0.49}4d^{9.80}5p^{0.13}$
7	−1.063	0.626	$2s^{1.48}2p^{4.56}3p^{0.01}3d^{0.01}$	$5s^{0.39}4d^{9.83}5p^{0.15}$
8	−1.068	0.608	$2s^{1.49}2p^{4.56}3p^{0.01}3d^{0.01}$	$5s^{0.47}4d^{9.80}5p^{0.11}$
9	−1.094	0.575	$2s^{1.49}2p^{4.58}3p^{0.01}3d^{0.01}$	$5s^{0.57}4d^{9.70}5p^{0.16}$
10	−1.079	0.638	$2s^{1.49}2p^{4.57}3p^{0.01}3d^{0.01}$	$5s^{0.43}4d^{9.82}5p^{0.11}$
11	−1.067	0.598	$2s^{1.49}2p^{4.56}3p^{0.01}3d^{0.01}$	$5s^{0.48}4d^{9.80}5p^{0.12}$
12	−1.073	0.628	$2s^{1.49}2p^{4.56}3p^{0.01}3d^{0.01}$	$5s^{0.44}4d^{9.82}5p^{0.11}$
13	−1.066	0.597	$2s^{1.48}2p^{4.56}3p^{0.01}3d^{0.01}$	$5s^{0.49}4d^{9.80}5p^{0.12}$
14	−1.057	0.469	$2s^{1.48}2p^{4.55}3p^{0.01}3d^{0.01}$	$5s^{0.60}4d^{9.79}5p^{0.15}$
15	−1.066	0.605	$2s^{1.49}2p^{4.56}3p^{0.01}3d^{0.01}$	$5s^{0.46}4d^{9.81}5p^{0.13}$

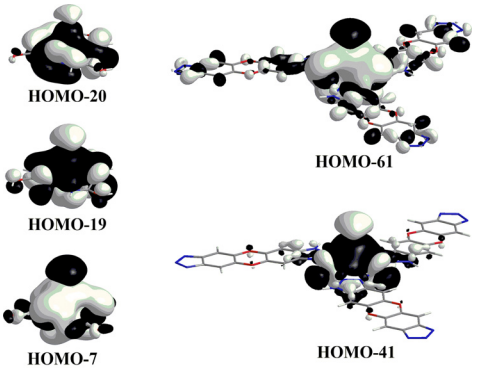

Fig. 6 3D surfaces of bonding MOs relevant to ammonia–silver cluster interactions in complexes **3** and **10**.

modulate D_0. Tables S2 and S3 (ESI†) present the values of a series of parameters related to the molecular structure of the systems under study. These parameters are the quadrupole moments, Q_{xx} and Q_{zz}, the energies of the frontier MOs, E_{HOMO} and E_{LUMO}, the chemical potential, μ, the hardness, η, the electrophilicity, ω, the electronegativity, χ, and the polarizability, α. Parameters μ, η, ω and χ were calculated according to the following eqn (1)–(4):[50]

$$\mu = -(E_{HOMO} + E_{LUMO})/2 \quad (1)$$

$$\mu = -\chi \quad (2)$$

$$\eta = (E_{LUMO} - E_{HOMO})/2 \quad (3)$$

$$\omega = \mu^2/2\eta \quad (4)$$

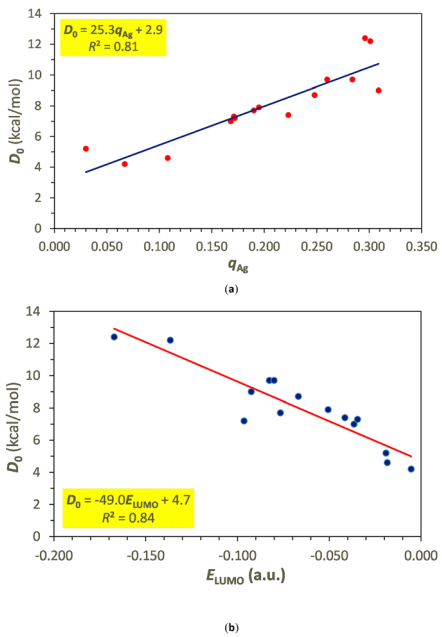

Fig. 7 Linear correlations of D_0 *versus* (a) the Mulliken charge, q_{Ag}, of complexes and (b) E_{LUMO} of the metallic clusters.

In addition, other parameters include the Mulliken and NBO charges on the Ag metal centres of clusters (Table S2, ESI†) and complexes (Table S3, ESI†) as well as on the N atom, q_N, of ammonia in complexes. For the latter, the dipole moment, p, of the complexes is also included in Table S3 (ESI†). Fig. 7 depicts the two best correlations found namely D_0 *versus* q_{Ag} of the complexes with NH_3 and *versus* E_{LUMO} of the 'free' clusters.

The linear correlations depicted in Fig. 7 indicate that the strength of the interaction of NH_3 with the metal ring increases as the positive charge on silver metal centres increases. This reflects the electrostatic nature of the interaction. On the other hand, the lower the LUMO energy of the cluster the stronger its interaction with NH_3. This implies the favourable HOMO–LUMO interaction between the HOMO of NH_3 and the LUMO of the 'free' clusters (see Fig. S4, ESI†).

4. Conclusions

In the present study, we introduce for the first time, a novel type of intermolecular interaction between NH_3 and the metallic ring of Ag(I) cyclic trinuclear clusters, *cyclo*-$Ag_3(\mu_2\text{-}L)_3$. The most favourable orientation is that with the N atom of NH_3 facing the trinuclear metallic ring and bridging the three Ag(I) metal centres. A multitude of methods have been employed in order to delineate the nature of the novel interaction namely AIM, RDG, NBO and MEP. It is found that the interaction of NH_3 with the Ag(I) clusters in the *cyclo*-$[Ag_3(\mu_2\text{-}L)_3(\mu_3\text{-}NH_3]$ complexes is mainly of the ionic/electrostatic nature also with a small contribution from van der Waals forces. The covalent interactions are expected to be negligible while there is no charge transfer. Taking into account that the strength of the proposed novel type of interaction is in the range of 4–13 kcal mol^{-1}, it could be possibly utilized for ammonia storage in solid state materials such as MOFs. Finally, taken the significance of the noncovalent interactions of the $[NH_4]^+$ cation in biological systems[51] we indent to expand our studies on its interactions with all metal rings.

Conflicts of interest

There are no conflicts to declare.

References

1 G. A. Jeffrey and W. Saenger, *Hydrogen Bonding in Biological Structures*, Springer-Verlag, Berlin, 1991.
2 G. R. Desiraju and T. Steiner, *The Weak Hydrogen Bond in Structural Chemistry and Biology*, Oxford University Press, New York, 1999.
3 A. Karshioff, *Non-convalent Interactions in Proteins*, Imperial College Press, Singapore, 2006.
4 E. A. Meyer, R. K. Castellano and F. Diederich, Interactions with Aromatic Rings in Chemical and Biological Recognition, *Angew. Chem., Int. Ed.*, 2003, **42**, 1210.

5 L. M. Salonen, M. Ellermann and F. Diederich, Aromatic Rings in Chemical and Biological Recognition: Energetics and Structures, *Angew. Chem., Int. Ed.*, 2011, **50**, 4808.
6 G. R. Desiraju, Crystal Engineering: From Molecule to Crystal, *J. Am. Chem. Soc.*, 2013, **135**, 9952.
7 G. R. Desiraju, Crystal Engineering: A Holistic View, *Angew. Chem., Int. Ed.*, 2007, **46**, 8342.
8 J.-M. Lehn, *Supramolecular Chemistry: Concepts and Perspectives*, VCH, Weinheim, 1995.
9 J. W. Steed and J. L. Atwood, *Supramolecular Chemistry: A Concise Introduction*, John Wiley & Sons Inc., New York, 2000.
10 C. B. Aakeroy and K. R. Seddon, The hydrogen bond and crystal engineering, *Chem. Soc. Rev.*, 1993, **22**, 397.
11 S. Scheiner, *Hydrogen bonding, A theoretical perspective*, Oxford University Press, Oxford, 1997.
12 C. R. Martinez and B. L. Iverson, Rethinking the term ''pi-stacking'', *Chem. Sci.*, 2012, **3**, 2191.
13 J. C. Ma and D. A. Dougherty, The Cation–π Interaction, *Chem. Rev.*, 1997, **97**, 1303.
14 B. L. Schottel, H. T. Chifotides and K. R. Dunbar, Anion-π interactions, *Chem. Soc. Rev.*, 2008, **37**, 68.
15 Y. Kodama, K. Nishihata, M. Nishio and N. Nakagawa, Attractive interaction between aliphatic and aromatic systems, *Tetrahedron Lett.*, 1977, **18**, 2105.
16 M. Nishio, M. Hirota and Y. Umezawa, The CH/π Interaction. Evidence, *Nature, and Consequences*, Wiley-VCH, New York, 1998.
17 S. Tsuzuki, K. Honda, T. Uchimaru, M. Mikami and K. Tanabe, Origin of the Attraction and Directionality of the NH/π Interaction: Comparison with OH/π and CH/π Interactions, *J. Am. Chem. Soc.*, 2000, **122**, 11450.
18 S. Vaupel, B. Brutschy, P. Tarakeshwar and K. S. Kim, Characterization of Weak NH−π Intermolecular Interactions of Ammonia with Various Substituted π-Systems, *J. Am. Chem. Soc.*, 2006, **128**, 5416.
19 J. W. G. Bloom, R. K. Raju and S. E. Wheeler, Physical Nature of Substituent Effects in XH/π Interactions, *J. Chem. Theory Comput.*, 2012, **8**, 3167.
20 L. M. Salonen, M. Ellermann and F. Diederich, Aromatic Rings in Chemical and Biological Recognition: Energetics and Structures, *Angew. Chem., Int. Ed.*, 2011, **50**, 4808.
21 O. Takahashi, Y. Kohno and M. Nishio, Relevance of Weak Hydrogen Bonds in the Conformation of Organic Compounds and Bioconjugates: Evidence from Recent Experimental Data and High-Level *ab Initio* MO Calculations, *Chem. Rev.*, 2010, **110**, 6049.
22 P. Jurecka, J. Sponer, J. Cerny and P. Hobza, Benchmark database of accurate (MP2 and CCSD(T) complete basis set limit) interaction energies of small model complexes, DNA base pairs, and amino acid pairs, *Phys. Chem. Chem. Phys.*, 2006, **8**, 1985.
23 M. Egli and S. Sarkhel, Lone Pair−Aromatic Interactions: To Stabilize or Not to Stabilize, *Acc. Chem. Res.*, 2007, **40**, 197.
24 M. Egli and R. V. Gessner, Stereoelectronic effects of deoxyribose O4' on DNA conformation, *Proc. Natl. Acad. Sci. U. S. A.*, 1995, **92**, 180.
25 A. Reyes, L. Fomina, L. Rumsh and S. Fomine, Are water–aromatic complexes always stabilized due to π–H interactions? LMP2 study, *Int. J. Quantum Chem.*, 2005, **104**, 335.
26 S. K. Singh and A. Das, The n → π* interaction: a rapidly emerging non-covalent interaction, *Phys. Chem. Chem. Phys.*, 2015, **17**, 9596.
27 T. J. Mooibroek, P. Gamez and J. Reedijk, Lone pair–π interactions: a new supramolecular bond?, *CrystEngComm*, 2008, **10**, 1501.
28 A. C. Tsipis and C. A. Tsipis, Hydrometal Analogues of Aromatic Hydrocarbons: A New Class of Cyclic Hydrocoppers(I), *J. Am. Chem. Soc.*, 2003, **125**, 1136; C. A. Tsipis, E. E. Karagiannis, P. F. Kladou and A. C. Tsipis, Aromatic Gold and Silver 'Rings': Hydrosilver(I) and Hydrogold(I) Analogues of Aromatic Hydrocarbons, *J. Am. Chem. Soc.*, 2004, **126**, 12916; A. C. Tsipis and C. A. Tsipis, Ligand-Stabilized Aromatic Three-Membered Gold Rings and Their Sandwichlike Complexes, *J. Am. Chem. Soc.*, 2005, **127**, 10623; A. I. Boldyrev and L. Wang, All-Metal Aromaticity and Antiaromaticity, *Chem. Rev.*, 2005, **105**, 3716; A. N. Alexandrova, A. I. Boldyrev, H. Zhai, and L. Wang, Cu3C4−: A New Sandwich Molecule with Two Revolving C22- Units, *J. Phys. Chem. A*, 2005, **109**, 562.
29 S. M. Tekarli, T. R. Cundari and M. A. Omary, Rational Design of Macrometallocyclic Trinuclear Complexes with Superior π-Acidity and π-Basicity, *J. Am. Chem. Soc.*, 2008, **130**, 1669.
30 M. M. Olmstead, F. Jiang, S. Attar and A. L. Balch, Alteration of the Aurophilic Interactions in Trimeric Gold(I) Compounds through Charge Transfer. Behavior of Solvoluminescent $Au_3(MeN = COMe)_3$ in the Presence of Electron Acceptors, *J. Am. Chem. Soc.*, 2001, **123**, 3260.
31 M. A. Omary, M. A. Rawashdeh-Omary, M. W. Gonser, O. Elbjeirami, T. Grimes, T. R. Cundari, H. V. K. Diyabalanage, C. S. P. Gamage and H. V. R. Dias, Metal Effect on the Supramolecular Structure, Photophysics, and Acid−Base Character of Trinuclear Pyrazolato Coinage Metal Complexes, *Inorg. Chem.*, 2005, **44**, 8200; H. V. R. Dias, C. S. P. Gamage, J. Keltner, H. V. K. Diyabalanage, I. Omari, Y. Eyobo, N. R. Dias, N. Roehr, L. McKinney and T. Poth, Trinuclear Silver(I) Complexes of Fluorinated Pyrazolates, *Inorg. Chem.*, 2007, **46**, 2979; H. V. R. Dias and C. S. P. Gamage, Arene-Sandwiched Silver(I) Pyrazolates, *Angew. Chem., Int. Ed.*, 2007, **46**, 2192.
32 M. A. Omary, A. A. Mohamed, M. A. Rawashdeh-Omary and J. P. Fackler, Jr., Photophysics of supramolecular binary stacks consisting of electron-rich trinuclear Au(I) complexes and organic electrophiles, *Coord. Chem. Rev.*, 2005, **249**, 1372.
33 M. R. Haneline and F. P. Gabbaï, Electrophilic Double-Sandwiches Formed by Interaction of [Cp2Fe] and [Cp2Ni] with the Tridentate Lewis Acid [(o-C6F4Hg)3], *Angew. Chem., Int. Ed.*, 2004, **43**, 5471.
34 A. J. Rieth, Y. Tulchinsky and M. Dincă, High and Reversible Ammonia Uptake in Mesoporous Azolate Metal–Organic Frameworks with Open Mn, Co, and Ni Sites, *J. Am. Chem. Soc.*, 2016, **138**, 9401.

35 H. G. W. Godfrey, I. da Silva, L. Briggs, J. H. Carter, C. G. Morris, M. Savage, T. L. Easun, P. Manuel, C. A. Murray, C. C. Tang, M. D. Frogley, G. Cinque, S. Yang and M. Schröder, Ammonia Storage by Reversible Host–Guest Site Exchange in a Robust Metal–Organic Framework, *Angew. Chem., Int. Ed.*, 2018, **57**, 14778.

36 A. J. Rieth and M. Dincă, Controlled Gas Uptake in Metal–Organic Frameworks with Record Ammonia Sorption, *J. Am. Chem. Soc.*, 2018, **140**, 3461.

37 S. Moribe, Z. Chen, S. Alayoglu, Z. H. Syed, T. Islamoglu and O. K. Farha, Ammonia Capture within Isoreticular Metal–Organic Frameworks with Rod Secondary Building Units, *ACS Mater. Lett.*, 2019, **1**, 476.

38 C. Marsh, X. Han, J. Li, Z. Lu, S. P. Argent, I. da Silva, Y. Cheng, L. L. Daemen, A. J. Ramirez-Cuesta, S. P. Thompson, A. J. Blake, S. Yang and M. Schröder, Exceptional Packing Density of Ammonia in a Dual-Functionalized Metal–Organic Framework, *J. Am. Chem. Soc.*, 2021, **143**, 6586.

39 D. W. Kim, D. W. Kang, M. Kang, D. S. Choi, H. Yun, S. Young Kim, S. M. Lee, J.-H. Lee and C. S. Hong, High Gravimetric and Volumetric Ammonia Capacities in Robust Metal–Organic Frameworks Prepared via Double Post-synthetic Modification, *J. Am. Chem. Soc.*, 2022, **144**, 9672.

40 M. J. Frisch, G. W. Trucks, H. B. Schlegel, G. E. Scuseria, M. A. Robb, J. R. Cheeseman, G. Scalmani, V. Barone, B. Mennucci, G. A. Petersson, H. Nakatsuji, M. Caricato, X. Li, H. P. Hratchian, A. F. Izmaylov, J. Bloino, G. Zheng, J. L. Sonnenberg, M. Hada, M. Ehara, K. Toyota, R. Fukuda, J. Hasegawa, M. Ishida, T. Nakajima, Y. Honda, O. Kitao, H. Nakai, T. Vreven, J. A. Montgomery, Jr., J. E. Peralta, F. Ogliaro, M. Bearpark, J. J. Heyd, E. Brothers, K. N. Kudin, V. N. Staroverov, T. Keith, R. Kobayashi, J. Normand, K. Raghavachari, A. Rendell, J. C. Burant, S. S. Iyengar, J. Tomasi, M. Cossi, N. Rega, J. M. Millam, M. Klene, J. E. Knox, J. B. Cross, V. Bakken, C. Adamo, J. Jaramillo, R. Gomperts, R. E. Stratmann, O. Yazyev, A. J. Austin, R. Cammi, C. Pomelli, J. W. Ochterski, R. L. Martin, K. Morokuma, V. G. Zakrzewski, G. A. Voth, P. Salvador, J. J. Dannenberg, S. Dapprich, A. D. Daniels, O. Farkas, J. B. Foresman, J. V. Ortiz, J. Cioslowski and D. J. Fox, *Gaussian 09 (Revision-D.01)*, Gaussian, Inc., Wallingford CT, 2010.

41 J. P. Perdew, K. Burke and M. Ernzerhof, Generalized Gradient Approximation Made Simple, *Phys. Rev. Lett.*, 1996, **77**, 3865; M. Ernzerhof and G. Scuseria, Assessment of the Perdew–Burke–Ernzerhof exchange-correlation functional, *J. Chem. Phys.*, 1999, **110**, 5029; C. Adamo and V. Barone, Toward reliable density functional methods without adjustable parameters: The PBE0 model, *J. Chem. Phys.*, 1999, **110**, 6158.

42 F. Weigend and R. Ahlrichs, Balanced basis sets of split valence, triple zeta valence and quadruple zeta valence quality for H to Rn: Design and assessment of accuracy, *Phys. Chem. Chem. Phys.*, 2005, **7**, 3297; D. Rappoport and F. Furche, Property-optimized Gaussian basis sets for molecular response calculations, *J. Chem. Phys.*, 2010, **133**, 134105.

43 S. Grimme, S. Ehrlich and L. Goerigk, Effect of the damping function in dispersion corrected density functional theory, *J. Comput. Chem.*, 2011, **32**, 1456.

44 A. E. Reed, L. A. Curtiss and F. Weinhold, Intermolecular Interactions from a Natural Bond Orbital, Donor-Acceptor Viewpoint, *Chem. Rev.*, 1988, **88**, 899; F. Weinhold, in *The Encyclopedia of Computational Chemistry*, ed. P. V. R. Schleyer, John Wiley & Sons: Chichester, UK, 1998.

45 R. F. W. Bader, *Atoms in Molecules-A Quantum Theory*, Oxford University Press, Oxford, UK, 1990; R. F. W. Bader, *J. Phys. Chem. A*, 1998, **102**, 7314.

46 P. Wu, R. Chaudret, X. Hu and W. Yang, Noncovalent Interaction Analysis in Fluctuating Environments, *J. Chem. Theory Comput.*, 2013, **9**(5), 2226.

47 T. Lu and F. Chen, Multiwfn: A multifunctional wavefunction analyser, *J. Comput. Chem.*, 2012, **33**, 580.

48 E. R. Johnson, S. Keinan, P. Mori-Sánchez, J. Contreras-García, A. J. Cohen and W. Yang, Revealing Noncovalent Interactions, *J. Am. Chem. Soc.*, 2010, **132**, 6498.

49 E. Espinosa, I. Alkorta, J. Elguero and E. Molins, From weak to strong interactions: A comprehensive analysis of the topological and energetic properties of the electron density distribution involving X–H···F–Y systems, *J. Chem. Phys.*, 2002, **117**, 5529.

50 P. Geerlings, F. De Proft and W. Langenaeker, Conceptual Density Functional Theory, *Chem. Rev.*, 2003, **103**, 1793.

51 M. R. Davis and D. A. Dougherty, *Phys. Chem. Chem. Phys.*, 2015, **17**, 29262.

